Minimum Energy Consumption in Multicomponent Distillation: Part III: More than Three Products and Generalized Petlyuk Arrangements

Ivar J. Halvorsen[1] and Sigurd Skogestad*

Norwegian University of Science and Technology,

Department of Chemical Engineering, N-7491 Trondheim, phone +47 73594030, fax +47 73594080

1. Currently at SINTEF Electronics and Cybernetics, N-7465 Trondheim

Email: Ivar.J.Halvorsen@sintef.no Sigurd.Skogestad@chembio.ntnu.no

Revised for publication 24 June 2002

Abstract

We consider separation of ideal multicomponent mixtures with constant relative volatility and constant molar flows and at constant pressure. The exact analytical solution of minimum energy in a generalized Petlyuk arrangement for separation of N-component feed into M products has been derived. Interestingly, the minimum energy solution in a complex integrated Petlyuk arrangement is equal to the most difficult split between any pair of the products, as if each single split was to be carried out in an ordinary 2-product column. This extends the results for the 3-product Petlyuk arrangement from Part II to a generalized arrangement with any number of products and feed components. The solution is very simple to visualize in the V_{min}-diagram (Part I), simply as the highest peak. In addition, we obtain detailed flow rates and component distribution inside the arrangement. We also conjecture that the minimum energy requirement for the generalized extended Petlyuk arrangement is lower than the minimum energy requirement for any distillation configuration when we consider conventional adiabatic sections and no internal heat exchange. The V_{min}-diagram may thus be used to obtain a target value for the energy requirements.

Keywords: Petlyuk column, minimum energy, multicomponent separation

1 Introduction

What is the minimum energy requirement in multicomponent - multiproduct distillation? In this paper we present an analytical expression for minimum energy requirement for the separation of N feed components into M products (where normally $M \leq N$). We derive the expressions for a generalized extended Petlyuk arrangement, where all columns are directly (fully thermally) coupled. The assumptions are constant relative volatility, constant molar flows, constant pressure and infinite number of stages. We focus on a standard configuration shown in Figure 1. This configuration can be extended to any number of products by adding more arrays of directly coupled columns.

Analytical expressions for minimum energy in a ternary Petlyuk arrangement have been available for some time [1,2]. Carlberg and Westerberg[3,4] presented solutions for an arbitrary number of intermediate components. However, as mentioned by Christiansen[5], the general analytic solution of minimum energy for distillation of a multicomponent feed into multiple products have not been given in the literature for more than three products.

The extension to any number of products is the main result of this paper. This is a direct extension of the results for a 3-product Petlyuk column presented in Part II [6,7]. The derivation is based on the Underwood equations[8,9,10,11] and as in Part II we use the V_{min}-diagram to effectively visualize the minimum energy solution also for the generalized Petlyuk column with more than three products. The V_{min}-diagram was presented in Part I[12] and gives us a very simple tool to asses the properties of the solution. We obtain the detailed vapour flow requirement in all column sections for general multicomponent feeds and arbitrary product specifications. A review of the basic tools is given in Section 2.

The derivation of the minimum energy expression is divided into two parts. First, in Section 3, we deduce an analytical vapour flow rate expression for separation of N feed components into N pure products for the case when all internal columns are operated at their respective preferred splits[13], and we discuss some of its properties. Second, in Section 5 we verify that this solution is a minimum energy solution for the arrangement. Analytical expressions are only shown for sharp $M=N$ sharp split products. It is straightforward to apply the same approach

for nonsharp splits too. However, instead of presenting the more complicated analytic expressions we illustrate the general *M*-product case (*M*>*N*) with both sharp and nonsharp product split specifications by an example in Section 4.

Finally, in Section 6, we conjecture that the minimum vapour flow expression for the system in Figure 1 represent minimum energy for any possible distillation arrangement when we apply adiabatic column sections and no internal heat exchange in the system. The term adiabatic refers to a typical column section where there is no heat exchange along the section.

2 The Underwood Equations and the V_{min}-diagram

The Underwood equations, and in particular how the Underwood roots carry over to succeeding directly coupled columns[3] are the main keys to the analytical solution. In addition, we use the V_{min}-diagram to effectively visualize the exact analytical solutions. A brief description of the basic equations is given below.

Consider a two-product distillation column with a multicomponent feed (*F*) with liquid fraction *q* and composition vector *z* of *N* components. The net flow of components (w_i) are defined positive upwards and into feed junctions. The defining equation for the Underwood roots (ϕ) in the top and (ψ) in the bottom are:

$$\text{Top: } V_T = \sum_{i=1}^{N} \frac{\alpha_i w_{i,T}}{\alpha_i - \phi} \qquad \text{Bottom: } V_B = \sum_{i=1}^{N} \frac{\alpha_i w_{i,B}}{\alpha_i - \psi} \tag{1}$$

There will be *N* solutions for each root, and the sets from the top and bottom equations are generally different. By subtracting the equations above, we obtain what we denote the feed equation, which gives us the set of possible common roots θ:

$$V_T - V_B = \sum_{i=1}^{N} \frac{\alpha_i (w_{i,T} - w_{i,B})}{\alpha_i - \theta} = \sum_{i=1}^{N} \frac{\alpha_i z_i F}{\alpha_i - \theta} = (1-q)F \tag{2}$$

Underwood showed, that for ordinary columns, the number of each set of roots is equal to number of components *(N)*, and they obey: $\alpha_i \geq \phi_i \geq \theta_i \geq \psi_{i+1} \geq \alpha_{i+1}$, and there are *(N-1)* possible common roots. Furthermore, for the case with infinite number of stages, minimum vapour flow solutions corresponds to that pairs of Underwood roots in the top and bottom sections coincide with the common roots ($\phi_i = \theta_i = \psi_{i+1}$). This occurs only for the roots in the range between the relative volatility of the distributing components and we denote these *active roots.* Observe that all the possible common roots from (2) depend only on feed composition and quality, and not on how the column is operated.

2.1 The V_{min}-diagram

A two-product column has only two degrees of freedom in operation (e.g. *D* and *V*), and all possible operating points can be visualized in the *D*-*V* plane. This is the basic idea behind the V_{min}-diagram presented in Part I. For a given 4-component feed, an example is shown in Figure 2. Each peak and knot (P_{ij}) represent minimum vapour flow for sharp split between components *i* and *j*. The straight lines are distribution boundaries where one component is at the limit of being distributing. Inside each region, a particular given set of components are distributing and there is a corresponding set of active Underwood roots (θ). Thus, the exact component distribution can then be calculated from the equation set obtained by applying the active roots in (1). All the possible minimum energy solutions is found below the V_{min}-boundary (bold), and there is a unique solution for every feasible pair of key component recoveries. The peaks represent minimum energy operation for sharp split between adjacent components. For sharp split between components *j* and *j+1*, only one common Underwood (which obeys $\alpha_j < \theta_j < \alpha_{j+1}$) is active and the peak ($P_{j,j+1}$) can be expressed by:

$$P_{j,j+1}: \quad V_{Tmin}^{j/j+1} = \sum_{i=1}^{j} \frac{\alpha_i z_i F}{\alpha_i - \theta_j}, \qquad D^{j/j+1} = \sum_{i=1}^{j} z_i F \tag{3}$$

The preferred split (P_{AD} in Figure 2) is particularly interesting for directly coupled arrangements. Then all possible common roots are active. The characteristic of the preferred split is that it is the minimum energy solution when the heaviest component is removed from the top and the lightest component is removed from the bottom.

2.2 Carry Over Underwood Roots in Directly Coupled Columns.

In Part II we showed that the possible common Underwood roots in a directly coupled succeeding column are equal to the actual roots in the preceding column. For the arrangement in Figure 1 we have for column C21:

$$\theta_i^{C21} = \phi_i^{C1} \tag{4}$$

In C21 we only need to consider the roots between the relative volatilities of the components actually appearing at the feed junction. When column C1 is operated at its preferred split, all common roots in C1 are active and we simply obtain $\theta_i^{C21} = \theta_i^{C1}$. The possible common roots (θ) in C1 are given by the feed equation (2). (In the following we omit the superscript C1 for the roots of column C1).

For the arrangement in Figure 1, with the four feed components ABCD, we have 3 common roots in column C1 (θ_A, θ_B, θ_C). For C1 operated at its preferred split all of these roots will be active. Components ABC and the corresponding roots θ_A, θ_B will carry over to C21 and Components BCD and the roots θ_B, θ_C will carry over to C22. When both C21 and C22 are operated at their respective preferred splits, components AB will appear in the feed to C31 and θ_A carry over from C21. Similarly components BC and the root θ_B will appear in C32 and components CD and the root θ_C will appear in C33. This is indicated in Figure 3. The mixing of flows from C21 and C22 at the feed junction to C32 does not give any problems. It is shown in Halvorsen[7] that the liquid and vapour compositions are identical in the top of C22 and bottom of C21, and this is also confirmed by the simulation example in section 3.2.2

In Part II[6] it was shown that the carry over of the common Underwood roots from column C1 to the succeeding columns also implicate that the V_{min}-diagram for the succeeding columns overlap the diagram for the feed into the first column. Thus, this V_{min}-diagram contains information about all minimum flows in the succeeding columns, providing that all preceding columns is operated at the preferred split. This is illustrated in Figure 4.

3 Minimum Energy for N Components and N Products

We are now in position to compute the minimum vapour flow in a general extended Petlyuk arrangement with any number of feed components (*N*) and any number of products (*M*). We will start from the basic 4-product arrangement in Figure 3, which can be extended to any number of products by adding more sets of directly coupled columns. There is only one reboiler and condenser, always at the outlets for the final bottom and top products, respectively.

For an *M*-product arrangement, there are $M-1$ cross-sections that may have independent total vapour flow requirements through all intersected columns. These intersections represent the product splits in the system. We have chosen to use the particular set I1, I2 and I3 for $M=4$ which intersect all internal top sections as shown in Figure 3. Note that only the A-product pass through intersection I1, thus I1 represent the A/BCD split. I2 represent the AB/BC split since all of A and B but none of C and D pass here. Finally I3 represent the ABC/D split. This can easily be extended to the general M-product case.

When each internal column operates at its preferred split, all the common Underwood roots (θ_A,θ_B *and* θ_C for $N=4$) given by the feed equation (2) for the prefractionator feed will carry over to the succeeding columns as indicated in Figure 3.

Then, note that in each column section, cut by each intersection line (I1,I2 or I3), there is one common active Underwood root (e.g. θ_B is active in column C21 and C32 intersected by I2). We can apply this root in the defining equation for each column cross-section and find the total vapour flow through the intersections. For sharp product split, the net product flows are simply the amount of the main product component in the feed. The minimum vapour flow through I1 is trivially:

$$V_{min}^{I1} = \frac{\alpha_A w_{A,T}^{C31}}{\alpha_A - \theta_A} = \frac{\alpha_A z_A F}{\alpha_A - \theta_A} = V_{Tmin}^{C1,A/BCD} \tag{5}$$

We recognize that this is the same minimum energy as if the separation A/BCD was to be performed in a single column. At intersection I2 we know that all the light A component pass through the top of C21 too, and for the B-component we have $w_{B,T}^{C21} + w_{B,T}^{C32} = z_B F$. None of the heavier C and D components are present. The middle Underwood root (θ_B) is active in both C21 and C32, thus we have:

$$V_{min}^{I2} = \sum_{i=A,B} \frac{\alpha_i (w_{i,T}^{C21} + w_{i,T}^{C32})}{\alpha_i - \theta_B} = \sum_{i=A,B} \frac{\alpha_i z_i F}{\alpha_i - \theta_B} = V_{Tmin}^{AB/CD} \tag{6}$$

At I3 we know that all of components A, B and C are passing, but none of the heavy D. The root (θ_C) is active in all columns (C1, C22 and C33) and we get:

$$V_{min}^{I3} = \sum_{i=A,B,C} \frac{\alpha_i (w_{i,T}^{C1} + w_{i,T}^{C22} + w_{i,T}^{C33})}{\alpha_i - \theta_C} = \sum_{i=A,B,C} \frac{\alpha_i z_i F}{\alpha_i - \theta_C} = V_{Tmin}^{ABC/D} \tag{7}$$

Again we recognize these expressions as the vapour flow at the three peaks in the V_{min}-diagram for the pre-fractionator feed (3).

3.1 V_{min} for N Feed Components and N Pure Products

The results for the 4-components and 4-product system given above is easily extended to any number of products. Based on the same procedure we obtain that the maximum minimum vapour flow requirement through any horizontal cross-section in a generalized Petlyuk arrangement with N feed components and M=N pure products is found directly as the highest peak in the V_{min}-diagram for the feed.

The expression for a peak is given in equation (3), so if we relate the vapour to the top of the Petlyuk arrangement, the minimum vapour flow is given by:

$$\frac{V_{Tmin}^{Petl}}{F} = \max_j \left(\sum_{i=1}^{j} \frac{\alpha_i z_i}{\alpha_i - \theta_j} \right) \text{ for } j \in \{1, 2 \ldots, N-1\} \tag{8}$$

where the *N-1* common roots ($\theta_1 \ldots \theta_{N-1}$) are found by the feed equation (2).

Conclusion: T*he minimum energy solution for a generalized Petlyuk arrangement for N products and N feed components is given by the highest peak in the* V_{min}*-diagram.*

This is exactly the same as the most difficult binary split between two adjacent component groups in an ordinary 2-product distillation column.

The result directly generalizes what was shown for the 3-product Petlyuk column in Part II. In Section 4, we will show how to generalize this to any number of feed components (N) and products ($M \leq N$) with possibly nonsharp specifications. However, before we move on the general case, let us discuss some more properties of the solution by the following example.

3.2 Example: 4 components and 4 pure products

Feed data for this example is given as: *F=1, q=0.8, z=[0.25 0.25 0.25 0.25],* α*=[14, 7, 3, 1].* The feed composition (z_i), relative volatilities (α_i), and recoveries ($r_{i,T}$ in the table) are given for components A,B,C,D respectively.

3.2.1 Visualization in the V_{min}-Diagram

We have applied the general procedure from Part I (Halvorsen and Skogestad 2001a) for computing the numerical values for minimum energy for sharp split between each possible pair of key components (peaks and knots), and the results are given in Table 1:

Observe in Figure 4 how the vapour flow in each individual column in Figure 1 appear as a difference between the peaks and knots. Thus, for preferred split operation in each column, all internal flows and component recovery can be found from the data in Table 1. The relations are quite trivial and come from the material balance equations at the column junctions.

3.2.2 Composition Profile

A composition profile from a simulation example is shown in Figure 5. There are 30 stages in each column section (*N=60* in each column), and in practice this is close to infinite number of stages for this case (with purity requirements around 99.9%). The flow rates are taken from the V_{min}-diagram in Figure 4 and are applied directly in the simulator. This simulation is a practical confirmation of the analytical expressions for flows and pinch zones and for the minimum energy behaviour.

Observe the characteristic of a preferred split pinch zone at all feed junctions, and that one component is completely removed in the end of each column. Note also that the pinch zone composition in each column end is identical to the feed stage composition in the succeeding column. In each section, the compositions of the remaining components increase monotonously from the feed pinch to the end-pinch without any remixing. Note that if a column had its own reboiler and condenser, remixing at the end is inevitable.

4 General V_{min} for N Feed Components and M Products

For each extra product, we have to add another array of columns to the structure in Figure 3. The total number of internal directly coupled two-product columns to separate *M* products is: *(M-1)+(M-2)+...+2+1 = M(M-1)/2*. There are *M-1* product splits, and these can be related to *M-1* minimum energy operating points (peaks) in the V_{min}-diagram.

However, we have often more components (N) in the feed than number of products (M). Thus, we have to consider split between products, which may be specified as an aggregate of components. Fortunately, the characteristic of minimum energy operation is unchanged. Each internal two-product column should only separate the components belonging to the most extreme products in its feed (in terms of relative volatility).

For example, in the case of non-sharp separation of the light A in column C21, the expression for the vapour flow through intersection I1 becomes (ref. equation 5):

$$V_{min}^{I1} = \frac{\alpha_A w_{A,T}^{C31}}{\alpha_A - \theta_A} + \frac{\alpha_B w_{B,T}^{C31}}{\alpha_B - \theta_A} \quad (9)$$

Here we need to express the product specifications in terms of net flows (w) for the components appearing in each product stream. It is possible to continue with the other intersections and deduce the exact minimum energy expression equivalent to equation (8), but it is much more simple to illustrate the solution in a V_{min}-diagram as in the example below.

4.1 Example: 4 Products and 8 Feed Components

A V_{min}-diagram for M composite products can easily be drawn into the general N-component diagram. The procedure is similar; we compute the peaks and knots in the diagram from the minimum energy operation given by sharp split between each possible pair of products. Note that this does not mean sharp split between individual components if some components are allowed in more than one product.

In Figure 6 we illustrate for a given example how to use the V_{min}-diagram to assess minimum energy operation when M<N. The diagram (solid) is drawn for a given 8-component feed (ABCDEFGH) which shall be separated into four products (WXYZ) in an extended 4-product Petlyuk arrangement (Figure 3). The product specifications are given in Table 2. Based on these we can specify the required two degrees of freedom for each possible pair of product splits in a single two-product column. The resulting split specifications are given in Table 3, and the minimum energy solution for each split (I/J) gives us the peaks and knots (P_{IJ}) in the V_{min}-diagram for the M products shown (bold dashed) in Figure 6

The highest peak determines the maximum minimum vapour flow requirement in the arrangement. In this example this is the middle peak P_{XY}, which is directly related to column C32 (note that V_{Tmin}-values in Table 3 are for the given split in a two-product column, and that the required flow in the individual columns appear as we have shown in Figure 4). With a single reboiler, all the heat for vaporization has to be supplied in the bottom and since the other peaks are lower, columns C33 and C31 will get a higher vapour load than required. However, with

heat exchangers at the sidestream stage, we only have to supply heating for the requirement given by P_{YZ} in the bottom reboiler and heating for the difference between P_{YX} and P_{YZ} in the bottom of C32, which is at a lower temperature. We may also take heat out due to the difference between P_{XY} and P_{WX} above C32.

Observe that P_{XY} is of similar height as P_{AB}. This implies that we are able to separate the light component A as a pure product in the top with a similar vapour flow requirement as given by P_{XY}. Thus, we can see directly from the diagram that we may change specification of product W to be pure A without consuming any more energy (but then we cannot take out any heat above C32 of course).

The diagram also illustrates that non-sharp product specifications can be handled quite easily. Note how the peak P_{XY} follows the contour lines for $r_{E,T} = 0.1$ and $r_{D,T} = 0.9$.

The same example could be used for cases where M=N too.

As a last comment on our example, observe that the “preferred” split is at P_{WZ}. We put “preferred” in quotes since we have earlier defined the preferred split at minimum energy for the most extreme component split which would be A/H here. But since H never need to be separated from the other components, we do not need that split. Instead we only separate products W and Z in the prefractionator (C1), which really is a split between components A and G. Thus, we may say that P_{WZ} represents the preferred split for our four aggregate products.

5 Verification of the Minimum Energy Solution

In Section 3 we found the analytical expression for the vapour flow requirement for the generalized Petlyuk arrangement when all internal columns are operated at their respective preferred splits, but we have yet not proved that this expression really represents the minimum energy solution for the extended Petlyuk arrangement.

Here we formulate minimization of energy as an optimization problem and verify that the solution given in equitation (8) (the highest peak), really is optimal for the extended Petlyuk arrangement. We will do this by two steps. First by determining the feasible region of operation for the given product specifications, and second by showing that no changes in any degrees of freedom within the feasible region may reduce the minimum vapour flow requirement.

We will limit the presentation to *N* components and *M=N* pure products. However, the result will also be valid for the general case, e.g. the example in section 4 above.

5.1 Minimum Vapour Flow as an Optimization Problem

We formulate the criterion function as the maximum of the minimum vapour flow requirements through any of the intersections I1, I2,.... I(M-1).

$$J(u) = max(V^{I1}, V^{I2}, \ldots, V^{I(M-1)}) \tag{10}$$

Here *u* represents our degrees of freedom in operation, and we have in general two degrees of freedom for every column, e.g. expressed by (*D,V*) for each. Thus:

$$dim(u) = M(M-1) \tag{11}$$

The main constraints are given as the final product (*Pi*) specifications. We may also treat arrangements with a lower number of degrees of freedom, by specification of a set of flow constraints, expressed as the equality *g(u)=0*. An example is if we restrict the feed to column C32, in the 4-product column in Figure 1, to be a single liquid stream; then $g(u) = V_B^{C21} - V_T^{C22} = 0$ expresses the constraint.

With given feed properties, (*F,* α*, z, q*) and sharp product split specification, the optimization criterion can be expressed as:

$$J_{opt} = \min_{u} J(u)$$
$$\text{subject to constraints} \begin{pmatrix} r_i^{Pi} = 1 \\ r_i^{Pj} = 0 \qquad \forall (i \neq j) \\ g(u) = 0 \end{pmatrix} \tag{12}$$

Here P_i denote product number i.

5.2 Requirement for Feasibility

The feasible region is the operation region where we have fulfilled the operational constraints in (12). Here we only consider the pure products specifications, and no additional constraints (no $g(u)=0$).

Then feasible operation requires operation on, or above the *V*-shaped boundary in the V_{min}-diagram for each column. For example in the 4-component example, the feasible region for the prefractionator is on or above P_{AB}-P_{AC}-P_{AD}-P_{BD}-P_{CD}. Note that the V_{min}-diagram for the succeeding columns only overlap the prefractionator diagram when this is operated at its preferred split. In other cases we must find the new V_{min}-diagram for each column, given by the actual Underwood roots for the proceeding columns[12].

This is easy to show by the following argumentation for the 4-product column:

Assume first close to preferred split operation in all columns. Then change the operation of C1 so we allow some light A to be transported downwards in C1 and into C22. This A have to be transported upwards in C22 since it is more volatile than B which also is transported upwards, and then some amount of A have to be present at the feed junction to C32. A portion will have to enter C32, and since A still is more volatile than B, it will also be transported upwards in C32 and will appear in the product stream from the junction C31/C32 where we have specified a pure B product.

We may do this “experiment” with a sloppy split for any of C1, C21 and C22. In all these columns, the most heavy feed component for every column has to be fully removed in the top, and the most volatile have to be fully removed from the bottom in order to obtain sharp product splits in the final columns of the sequence.

5.3 Verification of The Optimal Solution

In the following we will show that it is not possible to obtain any reduction in minimum vapour flow by changing the operation in away from the preferred split (inside the feasible region).

An important characteristic of the direct coupling is that the actual Underwood roots in a column section (ϕ in tops and ψ in bottoms) carry over as a common root (θ) to the succeeding column (Halvorsen and Skogestad 2001b), (Carlberg and Westerberg 1989). We combine this with Underwood's minimum energy results which states that for a given column $\phi_i \geq \theta_i \geq \psi_{i+1}$.

Consider now the top of the 4-product arrangement. It is clear that the first roots in the columns C1, C21 and C33 have to obey:

$$\phi_A^{C31} \geq \theta_A^{C31} = \phi_A^{C21} \geq \theta_A^{C21} = \phi_A^{C1} \geq \theta_A^{C1} = \theta_A \tag{13}$$

The vapour flow in the top of C31 is generally expressed by ϕ_A^{C31}, thus we obtain:

$$V_T^{C31} = \frac{\alpha_A z_A F}{\alpha_A - \phi_A^{C31}} \geq \frac{\alpha_A z_A F}{\alpha_A - \phi_A^{C21}} \geq \frac{\alpha_A z_A F}{\alpha_A - \phi_A^{C1}} \geq \frac{\alpha_A z_A F}{\alpha_A - \theta_A} = V_{Tmin}^{A/B} \tag{14}$$

This expression shows that there is no way to operate columns C1, C21 or C31 so that the vapour flow requirement in the top of C31 is reduced below the minimum which is given by the peak P_{AB} in the V_{min}-diagram. The minimum solution is only obtained when we operate column C1 in a region where θ_A is active. This is only obtained along the curve P_{AD}-P_{AC} (really also along P_{AC}-P_{AB}, but then we remove component C and not only D in the top of C1, and then we might remove column C21 completely). In addition C21 must also keep θ_A active, which is obtained along P_{AC}-P_{AB}, and at last, C31 must be operated exactly at P_{AB}. This line of argumentation is easy to extend to the general N-component N-product case.

Operation of columns C22, C32 and C33 have no direct impact on P_{AB}, thus there is no way to operate these columns to reduce the peak P_{AB}. This shows that the peak P_{AB} represent the absolute minimum vapour flow for the top of the Petlyuk arrangement also for other operation points than preferred split for each internal column.

Similarly, in the bottom of columns C1, C22 and C33 we have:

$$\psi_D^{C31} \le \theta_C^{C33} \;=\; \psi_D^{C21} \le \theta_C^{C21} \;=\; \psi_D^{C1} \le \theta_C^{C1} \;=\; \theta_C \tag{15}$$

which gives:

$$V_B^{C33} \;=\; \frac{\alpha_D z_D F}{\psi_D^{C31} - \alpha_D} \ge \frac{\alpha_D z_D F}{\psi_D^{C21} - \alpha_D} \ge \frac{\alpha_D z_D F}{\psi_D^{C1} - \alpha_D} \ge \frac{\alpha_D z_D F}{\theta_C - \alpha_D} \;=\; V_{Bmin}^{ABC/D} \tag{16}$$

Thus, all the bottom columns have to be operate with θ_C active in order to keep the minimum requirement in the bottom of C31 at peak P_{CD}. For sharp split, this is only obtained for C1 along P_{AD}-P_{BD}, C22 along P_{BD}-P_{CD} and C33 at P_{CD}. Thus P_{CD} represents the minimum vapour flow in the bottom of the Petlyuk arrangement for any operation of the arrangement.

It is important to note that we have to operate column C1 exactly at its preferred split (P_{AD}) to avoid increased vapour requirements in C31 or C33. Thus operation of C1 in the region above the preferred split will increase the vapour requirement represented by the peaks P_{AB} or P_{CD}.

However, column C1 have no such direct impact on the middle peak P_{BC}. The only requirement is that the root θ_B is active, since this root has to carry over to C33 via both C21 and C22. This is trivial as long as both B and C are distributed to both products. However, it is a bit more complicated if C21 or C22 is operated outside the region where θ_B is active. Then the resulting root in C32 will be different from the corresponding root in C21 and the expression for the total flow through intersection I2 will be more complicated than for the case in equation (6).

Assume now that we keep the vapour flows and product splits constant in columns C1 and C22. Thus, any change in vapour flow through intersection I2 must come through the bottom of C32 so:

$$\Delta V_{min}^{I2} \;=\; \Delta V_{Bmin}^{C32} \tag{17}$$

This can be expressed by the common Underwood root in C32 and the amount of C-component into the feed junction of this column.

$$V_{Bmin}^{C32} = \frac{\alpha_C w_{C,F}^{C32}}{\theta_B^{C32} - \alpha_C} \tag{18}$$

When the product splits in C21 and C22 are kept constant, this vapour rate depends only on the behaviour of the common Underwood root in C32, which is given as the solution of its feed equation:

$$V_F^{C32} = \frac{\alpha_B w_{B,F}^{C32}}{\alpha_B - \theta^{C32}} + \frac{\alpha_C w_{C,T}^{C22} - w_{C,B}^{C21}}{\alpha_C - \theta^{C32}} = V_T^{C22} - V_B^{C21} \tag{19}$$

Note that the net component feed rates to C32 is given directly from the material balance at the junction: $w_{i,F}^{C21} = w_{i,T}^{C22} - w_{i,B}^{C21}$. We assume that C22 is operated at its preferred split. Thus θ_B is active in C22. In C21, we may have operation outside the active θ_B region, thus we have to use the actual root ψ_C. The right hand side of (19) can now be written as:

$$V_T^{C22} - V_B^{C21} = \frac{\alpha_B w_{B,B}^{C21}}{\alpha_B - \psi_C^{C21}} + \frac{\alpha_C w_{C,B}^{C21}}{\alpha_C - \psi_C^{C21}} + \frac{\alpha_B w_{B,T}^{C22}}{\alpha_B - \theta_B} + \frac{\alpha_C w_{C,T}^{C22}}{\alpha_C - \theta_B} \tag{20}$$

By careful inspection of the structure of the feed equation (19-20), we observe that we always have $\frac{\partial}{\partial \psi_C^{C21}} \theta_B^{C32} > 0$ and that the solution have to obey:

$$\theta_B \geq \theta_B^{C32} \geq \psi_C^{C21} \tag{21}$$

Thus, we have that for suboptimal operation of C21, the actual Underwood root ψ_C^{C21} decreases from its original optimal value $\psi_C^{C21} = \theta_B$. Due to the structure of equation (20), the important Underwood root θ_B^{C32} also decrease, and from equations (19) and (18) we see that the flow through the intersection I2 must increase.

We may similarly analyse the operation of C22 outside the region where θ_B is active, and get to the conclusion that this will also increase the vapour rate through the cross-section I2.

It is clear that this result is independent of any changes in distribution of B and C components from column C1, C21 and C32. For each distribution case, we may start with θ_B active in both C21 and C22. Then any operation outside the active region in either C21 or C22 or both, will lead to an increase in the required flow through intersection I2.

We have not carried out a detailed proof for the general N-component M-product case for other than the far left and right peaks. But we expect that this can be done by the same line of argumentation as we used to state that the middle peak cannot be reduced for any feasible operation of C21 and C22. Numerical evidence also supports this.

If any part in the sequence of columns is operated away from the preferred split, the vapour flow requirement in some of the cross-sections have to increase, in other words; one or more of the peaks related to the specified product splits have to increase. In general, if a column has its preferred split at P_{XY}, and is operated above this point, all succeeding columns with knots and peaks related to either X or Y will in general be affected. Any sub optimal operation somewhere in the arrangement cannot be recovered in the succeeding columns.

5.4 The Flat Optimality Region

When the peaks are of different height, we may operate some of the columns away from the preferred split as long as the highest peak is not affected, and the other peaks do not grow above this one. This give rise to "flat" regions in the plot for overall energy requirement, V_B^{Petl} , as function of the degrees of freedom.

We illustrate this by an example in Figure 7. Since P_{CD} is the highest peak, the optimality region for C1 is along P_{AD}-P_{BD}. However, somewhere the actual Underwood root in the top of C1 related to the AB-split will get a value which makes the peak P_{AB}' given by $\phi_{A,\,Bal}$ equal the peak P_{CD}. This line segment limits the optimality region for both column C1 and C21, and this is very similar to the result from the ternary case discussed in Part II.

Similarly, C22 has to be operated along P_{BD}-P_{CD}. This optimality region is limited by how C21 is operated, since both affect the cross-section I2 through the Underwood root (θ_B^{C32}) given by equation (19). In Figure 7 we have indicated the operation at P_{BD}. Then we may find the optimality region for C21 in the marked region above P_{AC}. Note how operation of C1 limits the lower part of the optimality region for C21 through the contour for constant ϕ_A through X.

6 Minimum Heat Supply for all Adiabatic Distillation Arrangements Without Internal Heat Exchange.

Petlyuk[14] showed that it is possible to device a reversible Petlyuk arrangement with zero lost separation work and thus requires minimum separation work compared to any other separation process.

However, it has also been conjectured that the *adiabatic* Petlyuk arrangement, where all the heat is supplied in the bottom reboiler at the maximum temperature, requires minimum energy for vaporization (V_{min}) compared to any other adiabatic distillation arrangement (without internal heat exchange). (We apply the term *adiabatic column* section, as used by Petlyuk et. al.[15], to denote a column section with constant molar flows and no heat exchange along the section. Thus, the directly coupled columns in Figure 1 and also typical conventional arrangements contain adiabatic sections). However, no proof has been found in the literature[16], except for the ternary case. For the ternary case Fidkowski and Krolikowski[17] showed that the 3-product Petlyuk arrangement always has a smaller vapour flow than any arrangements with side-strippers or side-rectifiers and they showed that these also performed better than the conventional direct and indirect split sequences.

For the generalized adiabatic Petlyuk arrangement in Figure 1, the minimum energy requirement for separation of a feed mixture of N_c components is given by equation (8). Note that all the heat can be supplied in the bottom reboiler and be removed in the top condenser, but, in some cases, some of the heat may be supplied or removed at the product outlets.

In the following we consider adiabatic column sections, and we conjecture that the adiabatic Petlyuk arrangement is indeed the best distillation arrangement when we regard the total requirement for vaporization at constant pressure, and when we do not consider any internal heat exchange within the arrangement.

6.1 Direct Coupling Gives Minimum Vapour Flow

First we will show that the direct (fully thermal) coupling minimises the vapour flow requirement through any column junction.

Let us consider a general junction at the top of the prefractionator (C1) and the succeeding column (C21) as illustrated in Figure 8. To simplify we assume a ternary feed, but similar results can be obtained for any number of components and at any junction in an arrangement.

We assume that the two degrees of freedom in column C1 (e.g. D^{C1}, V_T^{C1}) are fixed. In Halvorsen (2001) we showed that the composition in the recycle flow (L_T^{C1}) from C21 to C1 normally has no effect on the net component flows from C1 to C21. This is so unless a component which would have been removed in an ordinary column (with a condenser) is not introduced in the recycle flow to the directly coupled column. For reasonable operation of the system this will normally not be a problem.

At the interconnection to C21 we allow for supply or removal of heat (still with fixed D^{C1}, V_T^{C1}). This will then only affect the effective liquid fraction (q^{C21}) to column C21 and have no impact on the component flows (w_i^{C1}). Recall that direct coupling implies that the reflux in C1 is taken directly as a side-draw from C21 and that the vapour flow from C1 is fed directly to C21. In this case the external heat exchange is zero, and we obtain an equivalent liquid fraction given by:

$$q_{dc}^{C21} = 1 - V_T^{C1} / D^{C1} \tag{22}$$

Note that we always have $q^{C21} < 0$ with direct coupling, which is equivalent to a superheated vapour feed. Heat removal (e.g. a condenser) will increase q^{C21} and heat supply (superheater) will decrease its value.

The most important effect of the direct coupling is that the Underwood roots in the top of C1 "carry over" as the common (minimum energy) Underwood roots for C21. Thus, $\theta_A^{C21} = \phi_A^{C1}$, which is vital in the following analysis.

For a given operation of the first column (not necessarily at minimum energy), the vapour flow, and net component flows in the top can be related to a certain Underwood root (ϕ), here given by the defining equation in column C1 (we omit the superscript C1 on w and ϕ):

$$V_T^{C1} = \frac{\alpha_A w_A}{\alpha_A - \phi_A} + \frac{\alpha_B w_B}{\alpha_B - \phi_A} + \frac{\alpha_C w_C}{\alpha_C - \phi_A} \quad (\text{note } D^{C1} = \sum w_i) \tag{23}$$

Consider now any type of interconnection to the succeeding column (C21). At minimum energy operation in C21 the flow rates are determined by the component distribution and the common Underwood roots. Thus:

$$\begin{aligned} V_{Tmin}^{C21} &= \frac{\alpha_A w_A^{C21}}{\alpha_A - \theta_A^{C21}} + \frac{\alpha_B w_B^{C21}}{\alpha_B - \theta_A^{C21}} + \frac{\alpha_C w_C^{C21}}{\alpha_C - \theta_A^{C21}} \\ V_{Bmin}^{C21} &= \frac{\alpha_A (w_A^{C21} - w_A)}{\alpha_A - \theta_A^{C21}} + \frac{\alpha_B (w_B^{C21} - w_B)}{\alpha_B - \theta_A^{c21}} + \frac{\alpha_C (w_C^{C21} - w_C)}{\alpha_C - \theta_A^{C21}} \end{aligned} \tag{24}$$

The common Underwood roots can be found from the feed equation of C21 (25) and will depend on the external heat through the feed quality. The net component flow and net distillate flow in C1 are constants.

$$\frac{\alpha_A w_A}{\alpha_A - \theta^{C21}} + \frac{\alpha_B w_B}{\alpha_B - \theta^{C21}} + \frac{\alpha_C w_C}{\alpha_C - \theta^{C21}} = (1 - q^{C21}) D^{C1} \tag{25}$$

Note that for any reasonable operation of columns, all net component flows are positive in the top sections and negative in the bottom sections. This implies that the minimum vapour flow in the top section will increase as the common Underwood root increase and the vapour flow in the bottom section will decrease.

In the following we fix the operation of column C1 such that V_T^{C1} and all w_i, and thereby all ϕ_j are constant, and we want to find the value of the common Underwood root in C21 (θ_A^{21}) which minimize the maximum vapour flow rates through any of the intersections above or below the feed junction (see Figure 8):

$$\min_{\theta_A^{C21}}\left(\max(V^{I1}, V^{I2})\right) \text{ where} \tag{26}$$

$$V^{I1} = V_{Tmin}^{C21} \text{ and } V^{I2} = V_T^{C1} + V_{Bmin}^{C21} \tag{27}$$

A typical dependency of V^{I1} and V^{I2} as a function of θ_A^{21} is shown in Figure 8, and we see that the analytical solution is given by:

$$\arg\left(\min_{\theta_A^{C21}}\left(\max(V^{I1}, V^{I2})\right)\right) = \phi_A \tag{28}$$

Proof

For normal operating conditions, we have $\frac{dV^{I1}}{d\theta_A^{C21}} > 0$ and $\frac{dV^{I2}}{d\theta_A^{C21}} < 0$.

This implies that $\min\left(\max(V^{I1}, V^{I2})\right)$ is found when $V^{I1} = V^{I2}$.

By applying $\theta_A^{C21} = \phi_A$ in equations (23-27) we obtain $V^{I1} = V^{I2}$.

Q.E.D.

In conclusion, minimization of the vapour rate through any intersection (I1 or I2) is found when the common Underwood roots in column C21 equal the actual roots in the top section of C1. This is exactly what we obtain with a direct coupling. Note that the proof does not require the first column to be operated at minimum energy and that it is valid for any distribution of components in C1.

6.2 Implications for Side-Strippers and Side-Rectifiers

A direct implication of the result in Section 6.1 above is that arrangements with side-strippers (like in Figure 8 with a direct coupling) or side-rectifiers, will always have a lower total need for vaporization than the corresponding indirect split or direct split configurations. This was also shown by Fidkowski and Krolikowski [17] for the ternary case, but it is straightforward to extend the result in Section 6.1 to the general multicomponent case.

6.3 The Adiabatic Petlyuk Arrangement is Optimal

The result in Section 6.1 gives rise to the following conclusion:

We assume constant relative volatilities, constant molar flows, constant pressure and no internal heat integration. Then the generalized adiabatic Petlyuk arrangement has the lowest need for vaporization compared to any other adiabatic distillation arrangement for separation of an arbitrary feed mixture into its pure components.

This result is based on the simple argument that at any junction where we might consider another type of connection than the direct coupling, the required vapour flow through the junction, and thereby through a cross-section of the whole arrangement, will increase.

We have not presented a complete proof, so the above conclusion is a conjecture. However, for the ternary case, it has been proved by Fidkowski and Krolikowski[17], when considering conventional arrangements and side-strippers as alternative configurations.

A qualitative explanation is that the direct (full thermal) coupling can be regarded as ideal heat integration. For example when a side stripper configuration is used instead of an indirect split configuration, the direct coupling replaces a condenser (which in practice has an inevitable loss). This is probably the background for the term “full thermal coupling” used by many authors. However, here we use the term “direct coupling” which relates to that both the vapour and liquid flows are coupled directly between two columns. In addition, we obtain reversible mixing at the junctions when we keep the vapour and liquid flows in the junctions at equilibrium.

7 Discussion

7.1 Alternative Configurations

There exist a very large variety of possible realisations for extended Petlyuk arrangements[18], which are equivalent in terms of energy requirement. For example in a recent article[19] it is shown that for a 4-product column, sections can be arranged together in 32 different configurations. For the 5-product column the number is 448 configurations which are equivalent in terms of minimum energy requirement. There are of course many important differences, i.e. in how easy it is to set individual vapour and liquid flow rates in practice, how the column arrangement behaves for non-optimal operation, how easy it is to control, possibility for operation at more than one pressure level, practical construction issues, etc.

7.2 Practical Petlyuk Arrangements (4-product DWC).

In the Petlyuk arrangement in Figure 1 we assume that we can adjust the vapour and liquid flow individually in all columns. The more practical arrangement in Figure 9 is a bit less flexible since all the vapour flow has to come from the bottom reboiler, and similarly, the liquid flow comes from the top condenser. It will generally have a higher energy requirement although it may be the same in some cases (see example). Since we extract only liquid sidestream products, also in the junction into the feed of C32. We get a simpler configuration, which also may be implemented as a dividing wall column (DWC) in a single shell, as indicated in Figure 9b

However, operation is by no means simple and we still have 9 manipulated inputs left, and when 4 are used for product purity, there are 5 left. These must be set properly in order to achieve the optimal operation given by the highest peak in the V_{min}-diagram.

The cross-sectional area is usually designed for a maximum vapour load. We know that there may be large differences between each section, e.g in C31 from Figure 2. However, in cases where the peaks are similar, we know that the total vapour requirement is similar in any cross section (I1,I2 or I3). Thus as indicated in Figure 9b, the DWC can be implemented in a single shell with a constant diameter, and with quite different, but suitable cross-sectional areas for the internal columns. This is one issue which makes DWC implementations attractive.

We assume the same feed and V_{min}-diagram as in Figure 4. We start by determining the requirement of the prefractionator (C1). The original diagram is of course valid for C1 and we chose to operate C1 at its preferred split, which is at P_{AD}. Then all the common roots from C1 carry over to C21 and C22. However, in Figure 9 we have the restriction: $V_B^{21} = V_T^{22}$. Here column C22 controls the vapour requirement since $V_{Bmin}^{21} < V_{Tmin}^{22}$. Thus minimum vapour for column C21 is somewhere on the line between the points X,Y in Figure 10. First we try to operate C21 in X. Then the root θ_A carries over all the way to C31, and the vapour flow requirement will be given by P_{AB}. However, θ_B will not carry over to C22. Instead a larger root will carry over and the requirement for C32 will be given by $P"_{BC}$. But as illustrated in the figure, this gives a higher vapour flow requirement than P_{CD}, which was our original highest peak. However, here we may increase the net product flow from C21 and move operation to Z. In this case $V>V_{min}$ in C21, and none of the common roots are active. Both C31 and C32 will be affected, and the new minimum vapour requirements are given by P'_{AB} and P'_{BC} respectively. In this example, we get a resulting diagram where P_{CD} still is the highest peak, and the minimum vapour flow requirement for this less flexible Petlyuk arrangement is the same as the fully flexible arrangement. It is quite clear, however, that we may use another feed and find cases where the less flexible arrangement can never reach the minimum requirement of the fully flexible configuration. For example if the peak P_{CD} were at the same height as P_{BC} in Figure 10. Then either of the peaks P'_{AB} or P'_{BC} would be higher than the original three peaks for any operation of C21 along the line Y-Z.

In summary, the solution is still simple to find by the V_{min}-diagram, but we get new peaks for the columns where the preceding column cannot operate at its preferred split. This can be done accurately by Underwood's equations, but we can also look directly at the diagram and find an approximate solution graphically. Note how the peak P'_{AB} rise and P'_{BC} fall as the operation of C21 is moved on the line from X towards Y.

Another important lesson is that we may change operation in some parts of the arrangement within the optimality region, without affecting the highest peak. The extent of this region is dependent on how different the peaks are and the practical impact is that some of our degrees of freedom do not need to be set accurately, only within a certain range.

7.3 The Kaibel column or the "⊢ column"

The Kaibel column[20] is a directly coupled arrangement for separating 4 components as shown in Figure 11. The interesting part is the extra column section (C2x where $L=V$) for separating B/C in the main column. However, the sharp B/C split is performed already in the prefractionator (C1), so section C2x is really not needed, and can be replaced by heat-exchange between bottom of C21 and top of C22, denoted the "¾⊢ column" by (Christiansen 1997).

The minimum vapour flow requirement in the Kaibel column is always outperformed by the full Petlyuk arrangement in Figure 1. This is simple to see from the V_{min}-diagram (e.g. in Figure 2). In the Petlyuk arrangement, the overall vapour requirement is given by the highest peak. In the Kaibel column, C1 is not operated at the preferred split, but at a sharp B/C split, which is given by the middle peak (P_{BC}). If this is the highest peak, it is obvious that the Kaibel column requires a higher reboiler vapour rate, since it require this vapour rate for C1, and we must in addition have some vapour flow for the separation of C/D in the top of C22. If P_{BC} is not the highest peak, we observe that when C1 is operated at P_{BC}, none of the common roots θ_A and θ_B are active in C1 and cannot carry over to C21 or C22. Then, as shown in Section 5.3, the expressions for minimum vapour in each of C21 and C22 have to be higher than the peaks P_{AB} and P_{CD}.

However, in cases when the B/C split is simple (P_{BC} much lower than P_{AB} and P_{CD}), the difference in energy requirement can be small, and the simpler configuration may be preferable with respect to capital cost and more simple operation.

7.4 Required Number of Stages - Simple Design Rule

The proposed stage design for ternary Petlyuk arrangements given in Part II an be applied for the extended arrangements too. We can calculate the pinch zones in all junctions for all columns at preferred split. This is trivial when we know all flow rates and component distribution from the V_{min} diagram. Then a minimum number of stages (N_{min}) can be found from the Fenske equation for each section for a given impurity of the component to be

removed in that section. This impurity can be set according to the impurity requirement in the products. The simple design rule: $N \approx 2N_{min}$ will typically give a real minimum vapour flow (V_{Rmin}) in the range between 5-10% above V_{min} found for infinite number of stages, for the same separation.

This simple design rule may of course be adjusted by more rigorous column computations and cost functions.

7.5 Control

M-product columns will of course be more complicated than the more familiar ternary Petlyuk arrangements. However the characteristic of optimal operation is similar, and is given by keeping each individual column at its preferred split.

By keeping the impurities of the components to be removed in each section at setpoints fixed at small values we ensure that the operation is at the preferred split, even if we do not know the feed. The magnitude of the allowed impurity setpoints in intermediate columns should be set according to the allowed impurities in the final products.

7.6 Real Mixtures

The characteristic of the optimal solution, with the ideal assumptions about mixture and properties used in this paper, is that every internal column have to be operated at their preferred splits. However, this is most likely to be the characteristic of the optimal solution for real mixtures too. Then there will be pinch zones across every feed junction and in the end of the preceding column, as shown in the simulation example for the ideal case in Figure 5. The actual pinch zone compositions and the flow rates have to be calculated numerically since the relative volatilities and molar flows may change along the column sections. At the internal mixing junctions, e.g. at the feed junction to column C32 in Figure 1, we may get some losses due to that there may be different compositions of the flows into the junctions even for preferred split operation of every column. Thus the characteristic of

the real minimum energy solution may deviate a little from the ideal case, but it is expected to be close. It is also possible that some of the alternative configurations for the same number of products (ref. Section 7.4) may be a little better than the others for a particular case.

The Underwood roots will still carry over at the junctions, but due to the changes in relative volatility and molar flows, the actual Underwood roots at any cross-section will also vary along the column, even for minimum energy operation. This implies that the V_{min}-diagram for the succeeding columns will not exactly overlap the V_{min}-diagram for the feed to the first column. However, we expect that the final solution for the internal flows will not be very far from the ideal case as in the example illustrated in Figure 4.

8 Conclusion

We have shown that the minimum energy results for the 3-product Petlyuk arrangement can indeed be extended to general multicomponent-multi product Petlyuk arrangements. An exact analytical expression, which is based on the Underwood equations, have been derived. The solution is very simple to visualize in the V_{min}-diagram for the feed, given by the following rule:

The minimum total vapour flow requirement in a multi-component, multi-product Petlyuk arrangement, is determined by the highest peak in the V_{min}-diagram.

Alternatively, since the V_{min}-diagram originally just characterize a two-product column with a multicomponent feed, this may also be expressed as:

The minimum total vapour flow requirement in a multi-component, multi-product Petlyuk arrangement is the same as the required vapour flow for the most difficult split between two of the specified products if that separation is to be carried out in a single conventional two-product column.

Note that the rule above applies to any feasible product specifications, both in cases with equal number of feed components and products, and for any possible component grouping in the products in cases where the number of products is less than the number of feed components.

In addition to the overall vapour flow requirement, we find the individual vapour flow requirement for every column section, directly from the same diagram. The V_{min}-diagram is based on feed data only and was originally intended to visualize minimum energy regions and distribution regions for all possible operating points, in an ordinary two-product distillation column with multicomponent feed.

The characteristic of the optimal solution is that all internal columns are operated on their respective preferred splits. In general this requires that we can adjust two degrees of freedom in each internal column. However, practical arrangements with less degrees of freedom may also reach the same minimum vapour flow.

The results have been derived for ideal assumptions, but the main characteristics of the solution will be valid for real mixtures too.

Although arrangements with more than 3 products may be feasible, the results for general M product systems have mainly theoretical interest. The most important result is that we can find the minimum target value for the vapour flow required for separation of a multicomponent feed by distillation in directly coupled arrangements. It is important to note that we have assumed constant pressure, and that we have not considered any internal heat exchange inside the system.

The latter may as shown in Halvorsen[7], give some further energy savings.

9 References

(1) Fidkowski, Z. and Krolikowski, L. Thermally Coupled System of Distillation Columns: Optimization Procedure, *AIChE Journal,* Vol. 32, No. 4, 1986.

(2) Glinos, K.N. and Nikolaides, I.P. and Malone, M.F. New complex column arrangements for ideal distillation. *Ind. Eng. Chem. Process Des. Dev,* 1986, vol. 25, no 3, pp 694-699

(3) Carlberg, N.A. and Westerberg, A.W. Temperature-Heat Diagrams for Complex. Columns. 3. Underwood's Method for the Petlyuk Configuration. *Ind. Eng. Chem. Res.* Vol. 28, p 1386-1397, 1989.

(4) Carlberg, N.A. and Westerberg, A.W. Temperature-Heat Diagrams for Complex. Columns. 2. Underwood's Method for Side-strippers and Enrichers. *Ind. Eng. Chem. Res.* Vol. 28, p 1379-1386, 1989.

(5) Christiansen, A.C. "Studies on optimal design and operation of integrated distillation arrangements. *Ph.D thesis* , 1997:149, Norwegian University of Science and Technology (NTNU).

(6) Halvorsen I.J. and Skogestad S. Minimum Energy Consumption in Multicomponent Distillation, II: Three-product Petlyuk Arrangements. *Submitted for publication*, October 2001

(7) Halvorsen, I.J. Minimum Energy Requirements in Complex Distillation Arrangements. *NTNU Dr. ing. Thesis*, 2001:43. Available from the web page of Sigurd Skogestad, Dept. of Chemical Engineering at NTNU (May 2002: http://www.chembio.ntnu.no/users/skoge/publications/thesis/2001/halvorsen/)

(8) Underwood, A.J.V. et. al. Fractional Distillation of Ternary Mixtures. Part I. *J. Inst. Petroleum*, 31, 111-118, 1945

(9) Underwood, A.J.V et. al. Fractional Distillation of Ternary Mixtures. Part II. *J. Inst. Petroleum*, 32, 598-613, 1946

(10) Underwood, A.J.V. Fractional Distillation of Multi-Component Mixtures - Calculation of Minimum reflux Ratio . *Inst. Petroleum*, 32, 614-626, 1946

(11) Underwood, A.J.V. Fractional Distillation of Multi-Component Mixtures. *Chemical Engineering Progress*, Vol. 44, no. 8, 1948

(12) Halvorsen, I.J. and Skogestad S. Minimum Energy Consumption in Multicomponent Distillation, I: Vmin-diagram for a two-product column. *Submitted for publication*, October 2001

(13) Stichlmair, J. Distillation and Rectification, *Ullmann's Encyclopedia of Industrial Chemistry*, B3, 4-1 -4-94, VCH, 1988

(14) Petlyuk, F.B., Platonov, V.M., Slavinskii, D.M. Thermodynamically optimal method for separating multi-component mixtures. *Int. Chem. Eng.* Vol. 5, No. 3, pp 555-561, 1965

(15) Petlyuk, F.B., Platonov, V.M., Girsanov, I.V. The design of optimal rectification cascades. *Khim. Prom.* No. 6, 45 (445)-53 (453), 1964.

(16) Petlyuk, F.B. Private communication 2000. ,

(17) Fidkowski, Z. and Krolikowski, L. Minimum Energy Requirements of Thermally Coupled Distillation Systems. *AIChE Journal,* Vol. 33, No. 4, pp6 43-653, 1987.

(18) Sargent, R.W.H. and Gaminibandara, K. Optimum Design of Plate Distillation. *Optimization in Action (book), Academic Press,* London 1976

(19) Agrawal R. A method to Draw Fully Thermally Coupled Distillation Column Configurations for Multi-component Distillation. *Trans. IChemE,* Vol. 78, Part A, April 2000, pp 454-464

(20) Kaibel, G. Distillation Columns with Vertical Partitions. *Chem. Eng. Technol.* vol. 10, pp. 92-98. 1987

10 LIST OF FIGURES

Figure 9: Practical 4-product Petlyuk arrangements with some flow restrictions: We allow only liquid feed to C32 and liquid intermediate side products B and C.

Figure 10: Vmin-diagram for 4-component feed ABCD with the less flexible Petlyuk arrangement in Figure 9. Vertical arrows are vapour flow requirements in each column section. Feed data: z=[0.25 0.25 0.25 0.25], α=[14,7 ,3,1],q=0.8

Figure 11: The Kaibel arrangement for separation of a 4-component feed

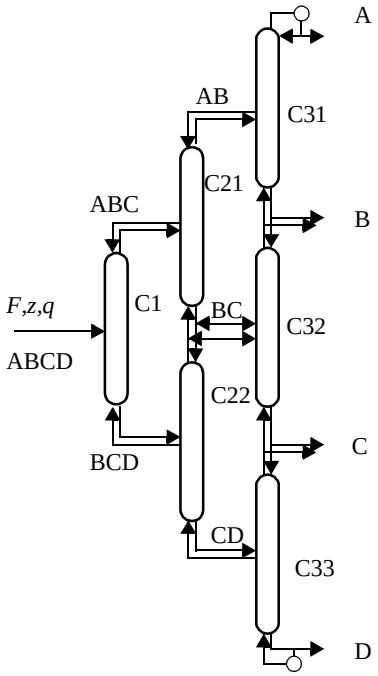

Figure 1: The Petlyuk arrangement extended to four products.
Vapour and liquid flow rates can be set individually in each internal 2-product column.

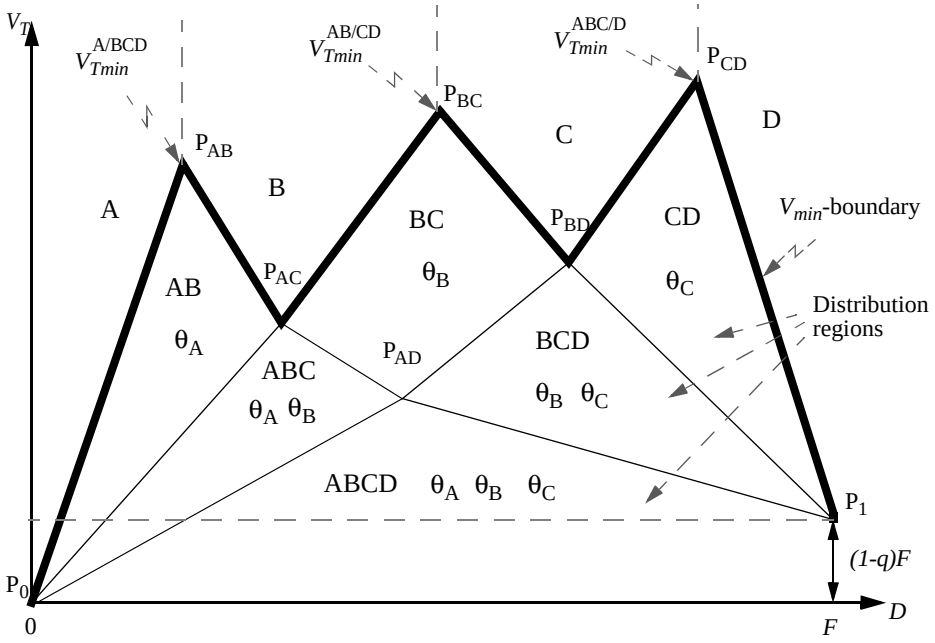

Figure 2: V_{min}-diagram for a given 4-component feed (ABCD) to the prefractionator. The set of distributed components and corresponding active Underwood roots are indicated in each distribution region. The preferred split is at P_{AD}.

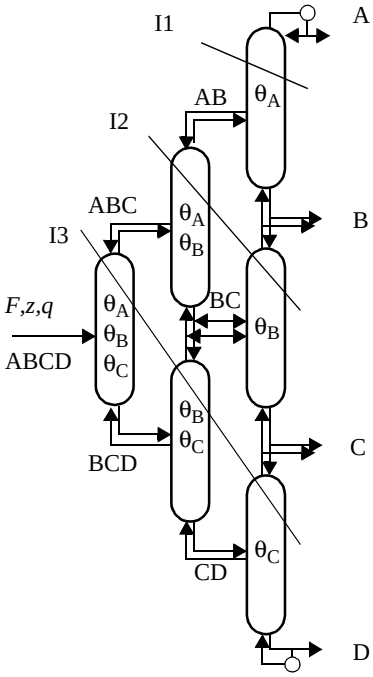

Figure 3: Extended 4-product Petlyuk Arrangement showing the active Underwood roots for preferred split operation of all internal columns.
The intersection lines represent the product splits (I1:A/BCD, I2:AB/CD, I3:ABC/D).

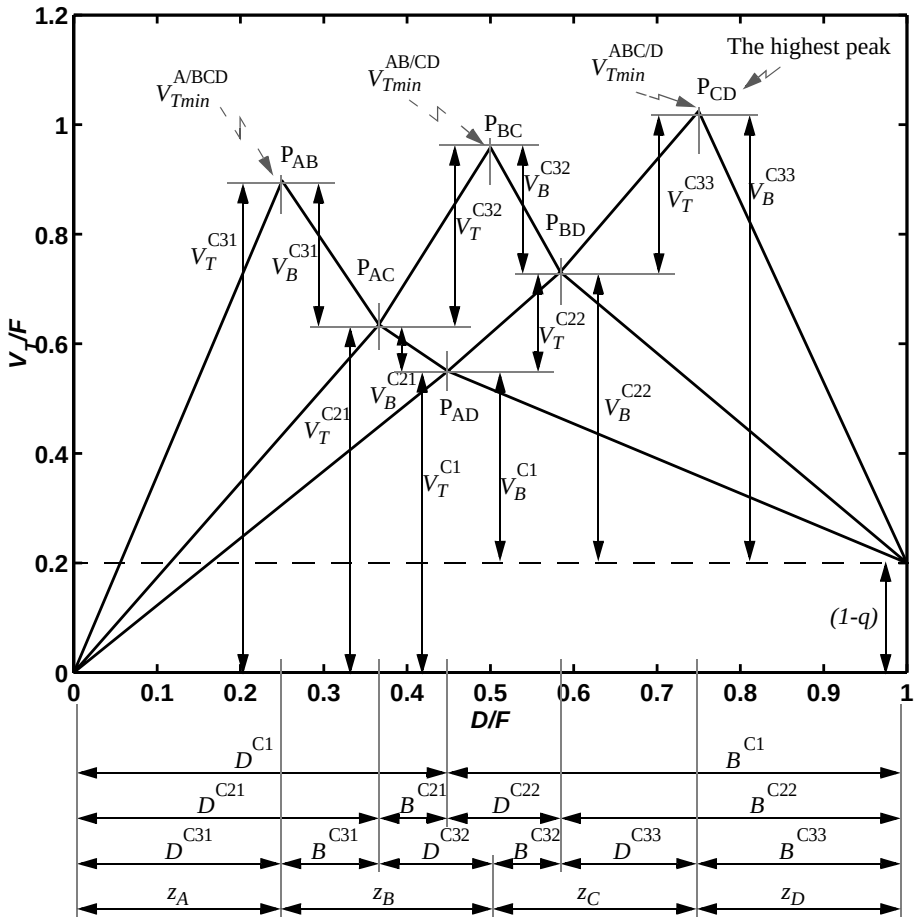

Figure 4: V_{min}-diagram showing the minimum vapour flows and product splits for every section in the Petlyuk arrangement in Figure 1 when each column C1, C21 and C22 operates at its preferred split (note that the subscript *min* should be on every vapour flow).

.

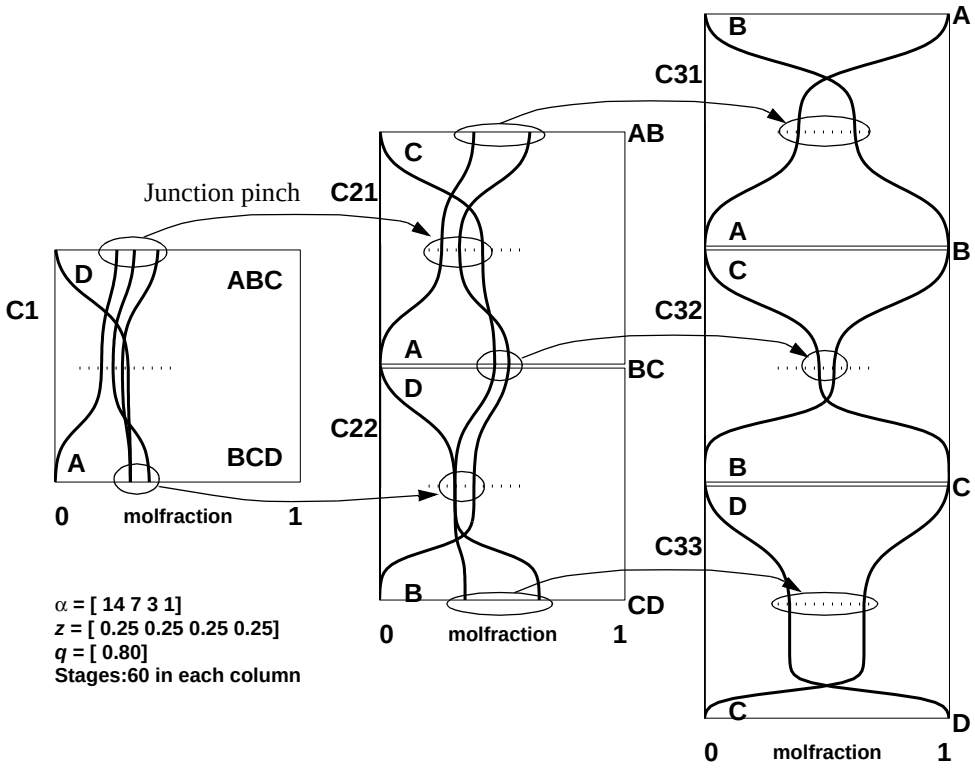

Figure 5: Composition profiles for the Petlyuk arrangement in Figure 1.
Each column is operated at its preferred split with vapour flows and product splits taken from Table 1 data as shown in the V_{min}-diagram in Figure 4. Observe the pinch zones in all junctions and how one component is removed in each column end.

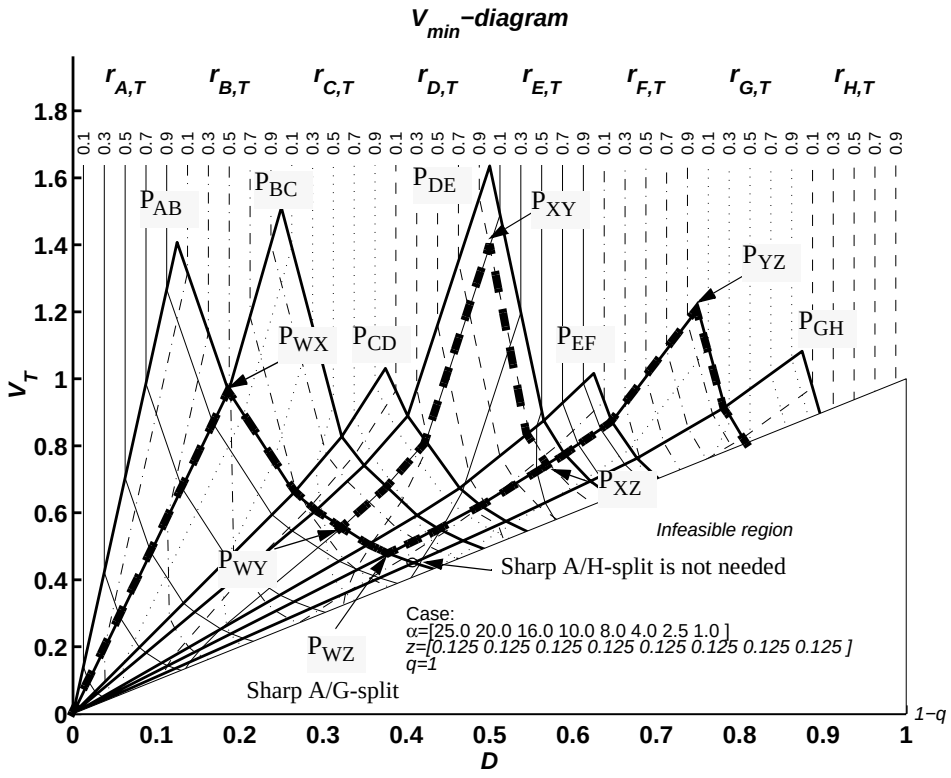

Figure 6: Assessment of minimum vapour flow for separation of a 8-component feed (ABCDEFGH) into 4 products (WXYZ). The plot shows the V_{min}-diagram for the feed components (solid) and the equivalent diagram for the products (bold dashed) is easily obtained from the product split specifications given in Tables 2 or 3.

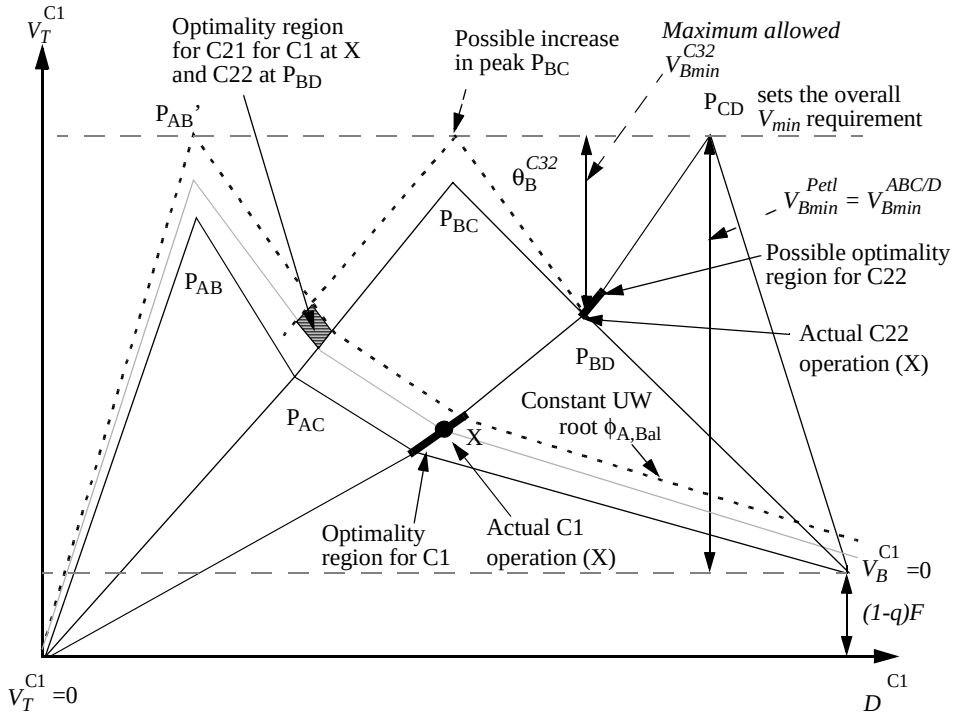

Figure 7: V_{min}-diagram for 4-component feed ABCD with optimality regions for operation of columns C1, C21 and C22. The contour lines for constant ϕ_A and a given constant θ_B^{C21} which makes $V^{A/BCD} = V^{AB/CD} = V_{min}^{ABC/D}$ are shown (dashed). These boundaries are the upper bounds for the optimality regions.

.

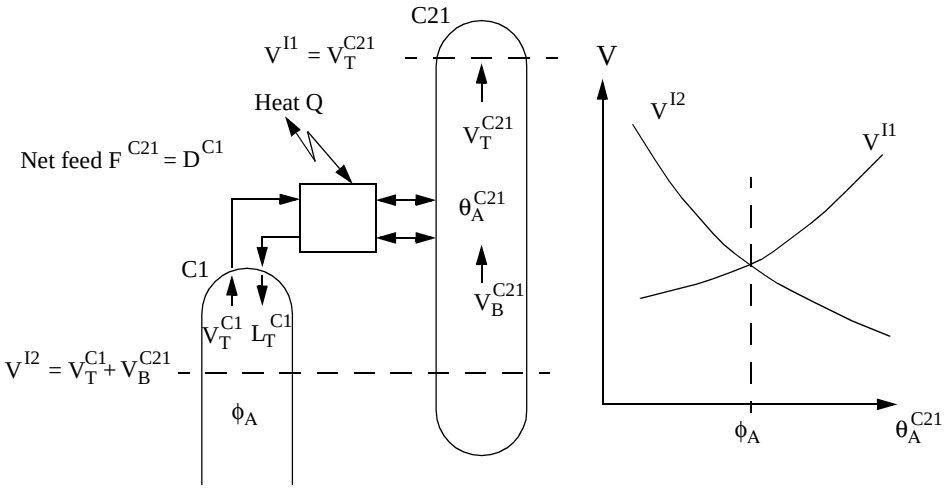

Figure 8: General column interconnection junction. The direct (full thermal) coupling gives $\theta_A^{C21} = \phi_A$ which implies $min(max(V^{I1}, V^{I2}))$ and a zero external heat exchange at the interconnection ($Q=0$).

.

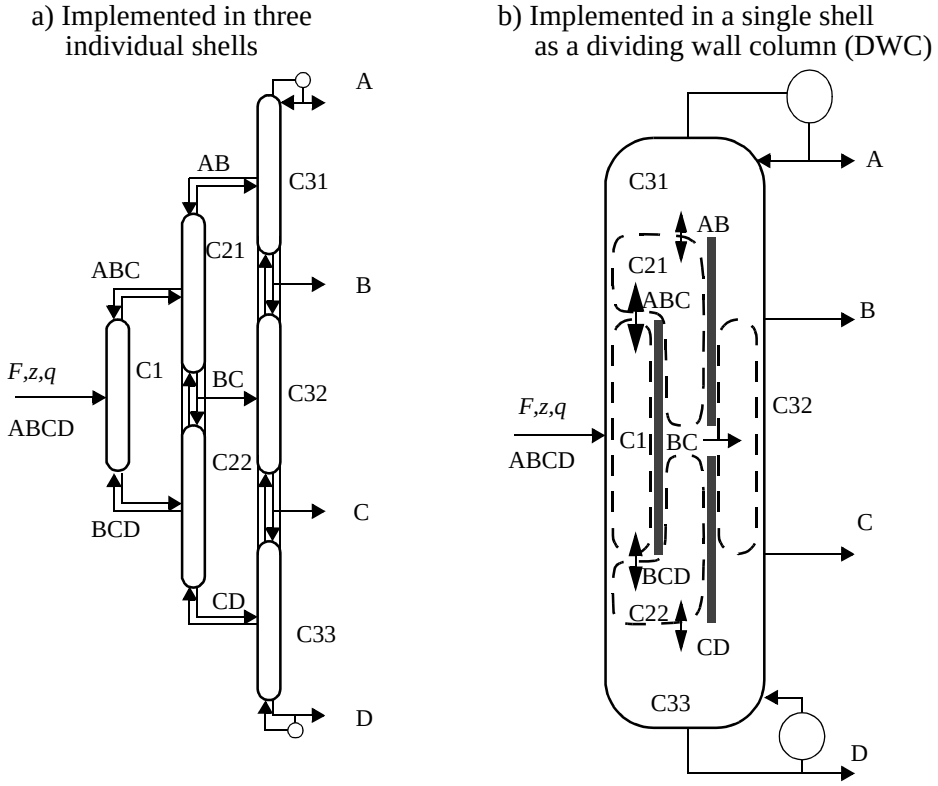

Figure 9: Practical 4-product Petlyuk arrangements with some flow restrictions:
We allow only liquid feed to C32 and liquid intermediate side products B and C.

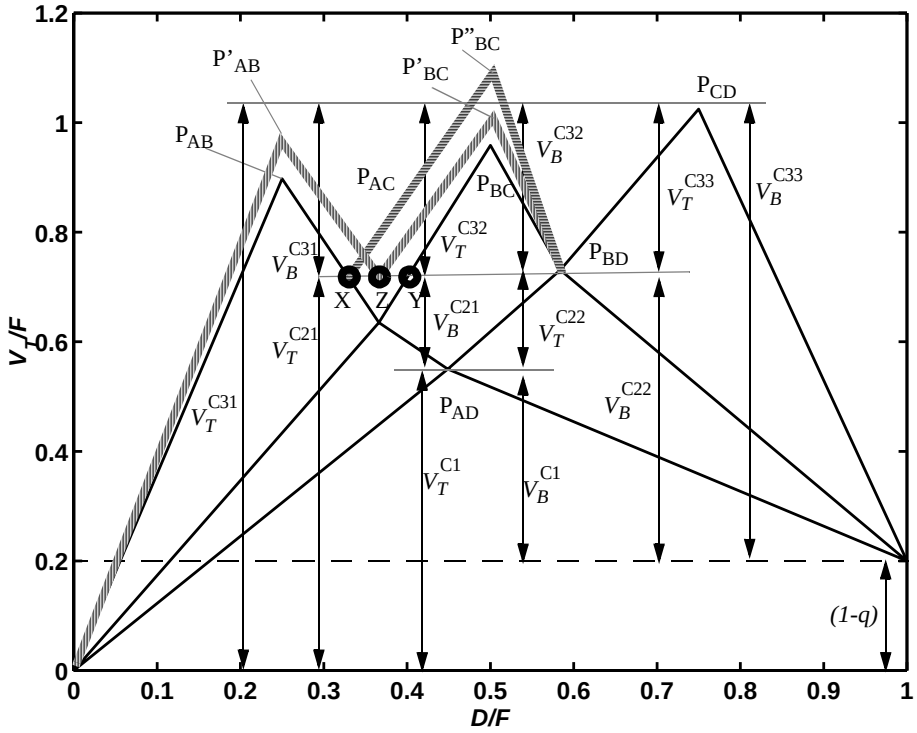

Figure 10: V_{min}-diagram for 4-component feed ABCD with the less flexible Petlyuk arrangement in Figure 9. Vertical arrows are vapour flow requirements in each column section. Feed data: *z=[0.25 0.25 0.25 0.25],* α*=[14,7 ,3,1],q=0.8*

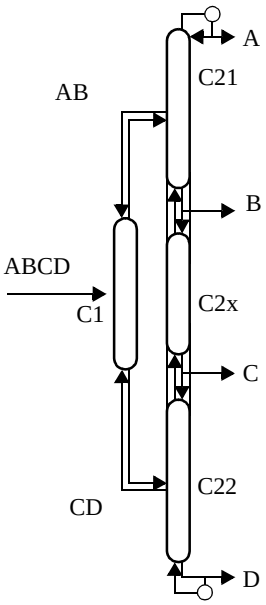

Figure 11: The Kaibel arrangement for separation of a 4-component feed

11 Tables

Table 1: Data for peaks and knots in the V_{min}-diagram

	P_{AB} sharp A/B	P_{BC} sharp B/C	P_{CD} sharp C/D	P_{AC} B distributing	P_{BD} C distributing	P_{AD} preferred split
V_{Tmin}	0.8975	0.9585	1.0248	0.6350	0.7311	0.5501
D	0.2500	0.5000	0.7500	0.3663	0.5839	0.4490
$r_{i,T}$	1,0,0,0	1,1,0,0	1,1,1,0	1,0.47,0,0	1,1,0.34,0	1,0.57,0.22,0

.

Table 2: Specification of feed component recoveries in products W,X,Y and Z.

Product	Light key impurity specification	Components	Heavy key impurity specification	Comment
W	-	A,B	0% C	all of A, any amount of B
X	0%A	B,C,D,E	<10% E	the rest of B
Y	<10.0%D	D,E,F	0% G	
Z	0% F	G,H	-	Sharp F/G split

Table 3: All possible product split specifications, by two key recoveries

Split	Col	Light key in top	Heavy key in top	V_{Tmin}	Comment
W/X	C31	100% A	0% C	0.9632	Sharp A/C split, B distributes.
X/Y	C32	>90% D	<10% E	1.3944	Nonsharp D/E split
Y/Z	C33	100% F	0% G	1.2093	Sharp F/G split
W/Y	C21	100% A	<10% E	0.5569	Sharp bottom, nonsharp top
X/Z	C22	>90% D	0% G	0.7477	Nonsharp top, sharp bottom
W/Z	C1	100% A	0% G	0.4782	“Preferred split” A/G, not A/H